Neurobiology of Disease 127 (2019) 374–381

Contents lists available at ScienceDirect

Neurobiology of Disease

journal homepage: www.elsevier.com/locate/ynbdi

Fast ripple analysis in human mesial temporal lobe epilepsy suggests two different seizure-generating mechanisms

Jan Schönberger[a,b,c,*], Birgit Frauscher[a], Nicolás von Ellenrieder[a], Massimo Avoli[a], François Dubeau[a], Jean Gotman[a]

[a] Montreal Neurological Institute and Hospital, McGill University, 3801 University Street, Montreal H3A 2B4, QC, Canada
[b] Universitätsklinikum Freiburg, Klinik für Neuropädiatrie und Muskelerkrankungen, Mathildenstraße 1, 79106 Freiburg im Breisgau, Germany
[c] Universitätsklinikum Heidelberg, Zentrum für Kinder- und Jugendmedizin, Klinik Kinderheilkunde I, Sektion für Neuropädiatrie und Stoffwechselmedizin, Im Neuenheimer Feld 430, 69120 Heidelberg, Germany

ARTICLE INFO

Keywords:
Mesial temporal lobe epilepsy
Seizure classification
Seizure onset pattern
High-frequency oscillations
Fast ripples

ABSTRACT

Objective: The distinction of hypersynchronous (HYP) and low-voltage fast (LVF) onset seizures in mesial temporal lobe epilepsy (MTLE) is well established, but classifying individual seizures and patients is often challenging. Experimental work indicates a strong association of HYP with fast ripples (250–500 Hz) and of LVF with ripples (80–250 Hz). We aimed to investigate whether analysis of high-frequency oscillations can be useful for characterizing the process of seizure generation in human MTLE patients.

Methods: We retrospectively compared 19 HYP and 14 LVF onset clinical seizures from ten and six consecutive MTLE patients with a predominance of the respective pattern. Five-second intervals of stereotactic EEGs from the seizure onset zone were selected, each representing the onset of HYP and LVF, the corresponding pre-ictal periods and, after the large spikes of HYP onsets, the LVF-like pattern that frequently followed.

Results: Pre-ictal fast ripple density and rate were higher for HYP than for LVF seizures ($p < .05$). This association was also found for initial ictal segments ($p < .001$). Furthermore, fast ripple density and rate were higher during the LVF-like pattern after HYP spikes than during LVF without preceding HYP ($p < .01$). Ripple density and rate in contrast did not differ significantly ($p > .05$). Fast ripple ($p < .01$) and ripple ($p < .001$) amplitude was higher during the LVF-like pattern after HYP spikes when compared to LVF without preceding HYP.

Significance: Our findings indicate a clear connection between experimental findings and human epilepsy. The association of fast ripples with HYP suggests that out-of-phase firing of different pyramidal cell clusters contributes specifically to generation of these seizures, rather than to LVF onsets. Both during and immediately before seizures, fast ripple analysis may facilitate classification.

1. Introduction

Epileptic seizures are the key feature defining epilepsy (Fisher et al., 2005), and the impairment in patients' quality of life is strongly linked to them. A prerequisite for development of treatments tailored to the individual patient is to understand the mechanisms underlying seizure generation. Classification of seizure types is the first step in this process (Bragin et al., 2005a).

In mesial temporal lobe epilepsy (MTLE), which is currently the most frequent focal epilepsy (Tellez-Zenteno and Hernandez-Ronquillo, 2012), it is common to distinguish two groups of seizures based on their stereotactic EEG (SEEG) onset pattern: Hypersynchronous (HYP), sometimes referred to as ictal spiking or periodic spiking, and low-voltage fast (LVF) onset seizures (Spencer et al., 1992; Schuh et al., 2000; Perucca et al., 2014). The occurrence of the HYP pattern is associated with “classical” hippocampal sclerosis, as evidenced by histopathology (Spencer et al., 1992; Park et al., 1996; Velasco et al., 2000) or MRI (Ogren et al., 2009), and a focal seizure onset zone (SOZ) (Velasco et al., 2000) located in the hippocampus (Perucca et al., 2014). Patients with LVF onset conversely had a more diffuse neocortical atrophy (Ogren et al., 2009) and a rather widespread SOZ located in different temporal subregions. The two entities may however not be as sharply discernible as these findings suggest. A single patient often shows seizures of the two types and some studies have reported that

* Corresponding author at: Montreal Neurological Institute and Hospital, McGill University, 3801 University Street, Montreal H3A 2B4, QC, Canada.
E-mail address: jan.schoenberger@yahoo.de (J. Schönberger).

https://doi.org/10.1016/j.nbd.2019.03.030
Received 21 December 2018; Received in revised form 19 March 2019; Accepted 26 March 2019
Available online 27 March 2019
0969-9961/

patients can have a strong (Velasco et al., 2000) or weak (Frauscher et al., 2017) predominance of HYP or LVF onset seizures. Besides, the LVF pattern has been recorded in temporal and extratemporal regions but the HYP patterns clearly predominates in temporal regions (Spencer et al., 1992; Perucca et al., 2014). Comparison of interictal epileptiform discharges and HFOs from patients with predominantly HYP and LVF onset seizures revealed only minor differences (Frauscher et al., 2017). Interestingly, an increase in fast ripple power during a HYP onset seizure has been reported (Weiss et al., 2016), but this link has not been studied systematically. Moreover, the HYP pattern is frequently followed by an LVF-like pattern, and in a recent study, a clinically identified LVF onset was preceded by a HYP pattern that was only visible in a simultaneous microelectrode recording (Weiss et al., 2016). It would thus be desirable to know if there are additional parameters that improve characterization of individual seizures and patients.

Here, we investigated whether high-frequency oscillations (HFOs) might serve this purpose. HFOs are a promising marker of epileptogenicity (Zijlmans et al., 2009; Jacobs et al., 2010; Jacobs et al., 2009), but the majority of studies has focused on interictal data and seizures have only been investigated sporadically (Perucca et al., 2014; Jirsch et al., 2006). However, we can rely on thorough experimental work: Co-occurrence of HYP seizures and fast ripples had been reported almost two decades ago in the rat kainic acid model of MTLE (Bragin et al., 1999). More recently, this link was confirmed in the pilocarpine model, in which an association of LVF seizures with ripples was also demonstrated (Lévesque et al., 2012). Interestingly, corresponding HFO subtype rates were also increased during pre-ictal intervals, i.e. fast ripples before HYP and ripples before LVF seizures. Following optogenetic studies it has been hypothesized that the LVF pattern is initiated by synchronous inhibitory activity, whereas predominance of excitation leads to HYP discharges (Shiri et al., 2015; Shiri et al., 2016) (see (Avoli et al., 2016; Weiss et al., 2019) for a review). Thus, in summary, the HYP and LVF are the only two seizure onset patterns that have been modeled extensively in animals, yielding a concept of the cellular mechanisms underlying their generation.

It has also been suggested that HFOs per se reflect clearly discernible mechanisms at the cellular level. The two traditionally distinguished subtypes could be linked to two different modes of local neuronal activity: While ripples are largely due to rhythmic GABAergic currents (Ylinen et al., 1995; Klausberger et al., 2003; Schönberger et al., 2014) (see (Klausberger and Somogyi, 2008) for a review), fast ripples might rather mirror out-of-phase firing of different pyramidal cell clusters, each of them synchronized within itself (Foffani et al., 2007; Ibarz et al., 2010) (see (Jiruska et al., 2017) for a review). Differences in ripple or fast ripple expression between to the two types of seizure onset might thus indicate differences in underlying network mechanisms. To examine this hypothesis in human patients and thus bridge the gap between animal model and human data was the main goal of our study.

2. Methods

2.1. Patient selection

Our patient group largely resembled the one selected for a previous study comparing interictal discharges in patients with predominantly HYP and LVF onset seizures (Frauscher et al., 2017). In brief, we considered all patients with medically intractable MTLE (uni- and bilateral, lesional and non-lesional) who, as part of their evaluation for epilepsy surgery, had undergone SEEG recordings at the Montreal Neurological Hospital between November 2004 and February 2018. From those, we included subjects with > 75% and at least three clinical seizures of one type of onset, HYP or LVF, termed “HYP patients” and “LVF patients”. HYP onset seizures were defined by a low-rate (~ 0.5–2 per s), medium- to high-voltage spiking activity lasting over 5 s (Spencer et al., 1992; Perucca et al., 2014). For LVF onset seizures, a clearly visible low-voltage rhythmic activity over ~ 10 Hz, which could be preceded by a single spike or slow wave, was required (Bragin et al., 2005a; Memarian et al., 2015). Selection of patients was performed by a board-certified neurologist blinded to the purpose of this study. This study was approved by the Review Ethics Board at the Montreal Neurological Institute and Hospital, and written informed consent was obtained from all patients.

2.2. Seizure selection and definition of analyzed intervals

We excluded seizures that (1) were purely electrographic, (2) arose from the side contralateral to that of the habitual seizures, (3) arose less than one hour after a previous seizure or (4) were accompanied by a disconnection of recording equipment during one of the intervals selected for analysis. A maximum of three seizures per patient was included to minimize the risk that group results might predominantly reflect a few patients with many seizures. If more seizures fulfilled inclusion criteria, we selected those recorded at the end of the implantation period to minimize the possibly confounding effects of tissue irritation related to surgery and of antiepileptic medication, which had been tapered during the evaluation period in some patients.

We defined two 5 s intervals, one representing the pre-ictal and another representing the initial ictal period (Fig. 1A, B). Seizure onset was defined as the onset of either HYP or LVF according to the criteria specified above (see “Patient selection” for details) by two EEG reviewers, one of them a board-certified neurologist blinded to the purpose of this study. If the HYP pattern was followed by an LVF-like pattern (Spencer et al., 1992), which we termed “HYP-LVF”, the initial 5 s of these HYP-LVF sections were also analyzed as a third interval. We analyzed the HYP-LVF sections because it is sometimes considered that the HYP pattern is pre-ictal and that the seizure really starts with the subsequent LVF activity (Lévesque et al., 2012). LVF activity was sometimes quickly replaced or superimposed by another pattern within 5 s of onset, in which case the HYP-LVF or LVF section was shortened accordingly. If this occurred within the first second after onset, the HYP-LVF interval (HYP group) or the whole seizure (LVF group) was excluded to ensure that only “stable” patterns of at least one second duration were analyzed.

2.3. SEEG recordings and HFO identification

Based on their estimated value for clinical decision-making in the individual patient, at least two (anterior hippocampus and amygdala) and often three (additional posterior hippocampus) intracerebral electrodes had been implanted orthogonally through the second temporal circumvolution. SEEG was acquired using the Harmonie system (Stellate, Montreal, QC, Canada). Recordings were band-pass filtered from 0.3 to 500 Hz, and seizures were only included if SEEG had been sampled at 2 kHz.

HFOs were visually identified based on previously established procedures (Zijlmans et al., 2009; Jacobs et al., 2010; Zijlmans et al., 2011). In brief, we used the Harmonie Reviewer software to review bipolar montages of neighboring SEEG electrode contacts. The screen was vertically split, and finite impulse response-filtered traces were displayed at maximum temporal resolution (0.4 s on each half) to mark ripples (80–250 Hz) on the left and fast ripples (> 250 Hz) on the right. An event was only regarded as an HFO if consisting of at least four oscillatory cycles above baseline activity. Two events were regarded as distinct if separated by at least two non-HFO cycles. If HFOs occurred within 100 ms of seizure onset, they were also marked and included into analysis of the initial ictal interval. HFOs associated with spikes during the baseline segment were excluded to provide evidence of their presence irrespective of the possible filtering effect of sharp transients (Schönberger et al., 2014).

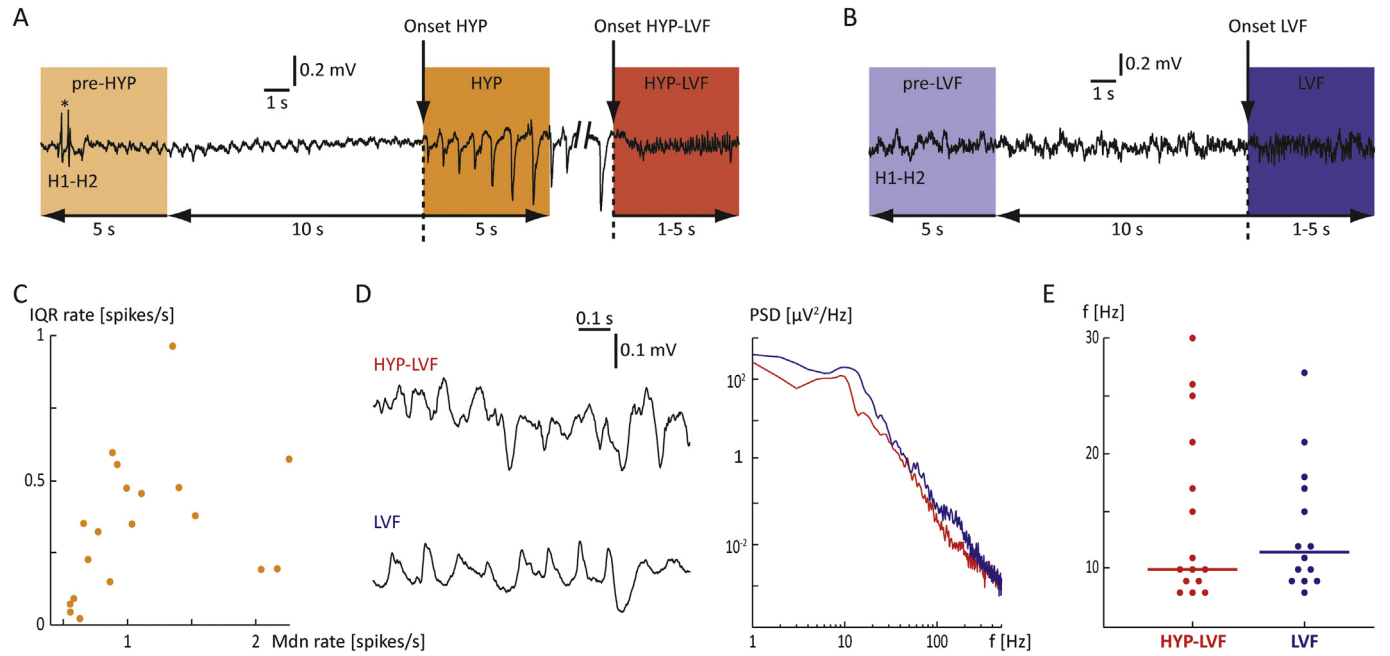

Fig. 1. Analyzed intervals, intra-group heterogeneity and inter-group similarity. (A, B) SEEG recording from the deepest hippocampal electrode bipolar channel of a representative HYP (A) and LVF (B) onset seizure. Intervals were defined as indicated. Pre-ictal spikes (*) were excluded from HFO analysis. (C) Seizure-specific median and interquartile range (IQR) of HYP spike rates, the latter being an indicator of periodicity. Each dot represents one seizure. Within the HYP group, a broad range from slow to fast and from more to less periodic patterns was observed. (D) (Left) One second interval of HYP-LVF (top) and LVF (bottom) from SEEG traces depicted in A and B, respectively. The two patterns appear very similar at first glance. (Right) Power spectral density estimates, computed for the whole HYP-LVF (top) and LVF (bottom) interval shown above. In this case, both patterns are characterized by a prominent peak at ~ 10 Hz. We usually found no distinct peak in the HFO frequency range (80–500 Hz). (E) LVF frequency, defined based on the power spectral density peak shown in (D). Each dot represents data from one seizure. We found a considerable spread inside the two LVF subgroups, and no significant difference between them (p = .86, Wilcoxon rank sum test).

2.4. Data analysis

Further computations were performed with custom-written routines in Matlab (Mathworks, Natick, MA). HYP spike rate was determined for each inter-spike interval (rate is inverse of inter-spike interval). For each HYP onset seizure, we could thus, in addition to a median rate, calculate a seizure-specific interquartile range (IQR) of rates to obtain an indicator of the periodicity of the HYP spikes. A low IQR indicates that events recur at more or less the same rate, whereas an irregular pattern results in a high IQR.

Power spectral density estimates were calculated to analyze the main frequency components of the EEG signal. We applied Welch's method, with segments of 0.5 s and a Hamming window of the same length. We thus obtained a frequency resolution of 2 Hz. The most prominent peak above or equal to 6 Hz was determined to estimate LVF frequency.

HFO density was defined as the percentage of time occupied by HFOs, as described previously (Perucca et al., 2014; Zijlmans et al., 2009). In seizures with HFOs, we also calculated HFO amplitude. This feature is not taken into account by traditional HFO parameters, such as rate, duration or frequency. “Ripple amplitude” was computed as follows: First, SEEG was band-pass filtered at 80–250 Hz. Zero-phase filtering was realized by application of a third order Butterworth infinite impulse response filter in forward and reverse directions. This signal was used during identified ripple intervals to calculate a subtype-specific root mean square (RMS), called “ripple amplitude” in this case. “Fast ripple amplitude” was similarly computed after 250–500 Hz band-pass filtering. For both HFO subtypes, we also calculated separate RMSs for intervals without HFO activity ($RMS_{non\text{-}ripple}$ and $RMS_{non\text{-}fast\ ripple}$). Finally, all of these variables were also computed after filtering the SEEG at 0.5–30 Hz, 30–80 Hz, 80–250 Hz and 250–500 Hz, and their ratios (RMS_{HFO} / $RMS_{non\text{-}HFO}$) compared.

2.5. Statistical hypothesis testing

The data was considered to be not normally distributed. Therefore we specified the median as a measure of central tendency and the range as a measure of dispersion. Seizure onset patterns frequently varied not only between, but also within individual patients, indicating that seizures from the same patient could be considered as - at least being close to – statistically independent. Therefore the Wilcoxon rank sum test was applied for unpaired data and a Wilcoxon matched-pairs signed-ranks test for paired data. For key findings we also performed a more conservative permutation test, which does not assume independence between seizures from the same subject (Table S1).

A significance level of 5% was chosen. The Holm-Bonferroni method was used to correct for multiple comparisons.

3. Results

3.1. Seizure and patient characteristics

Nineteen HYP onset seizures from ten patients (7 females, 3 males; age: median 35 years, range 21–60 years) and 14 LVF onset seizures from six patients (no females, 6 males; age: median 36, range 29–46 years) fulfilled inclusion criteria. The SOZ never extended beyond the three deepest electrode contacts, which were located in the mesial temporal structures, and was smaller in HYP than in LVF (HYP: median 3 channels, range 1–6 channels from 1 to 2 electrodes; LVF: median 6 channels, range 3–6 channels from 1 to 2 electrodes; p = .002, Wilcoxon rank sum test). A HYP-LVF pattern was observed after the hypersynchronous spikes in 15 of the 19 HYP onset seizures. Its duration did not differ significantly from the LVF without preceding HYP spikes (HYP-LVF: median 5.0 s, range 1.8–5.0 s; LVF: median 3.4 s, range 1.0–5.0 s; p = .06, Wilcoxon rank sum test).

3.2. Intra-group diversity of spike rate and spectral measures

Nine out of ten HYP patients (Table S2) and all six LVF patients (Table S3) had also been included in a previous study from our group (Frauscher et al., 2017). We consistently observed a pronounced diversity within these two classically defined groups - ranging from slower to faster and from rhythmic to rather chaotic variants. To quantify this observation, the HYP spike median rate and the IQR of spike rates as an indicator of spike periodicity were plotted for each HYP onset seizure (Fig. 1C; see above, "Data analysis" in the Methods section, for details). The diagram illustrates that within our HYP group, both spike rate and periodicity varied considerably, with only a weak correlation between them.

HYP-LVF and LVF could not be distinguished at first glance (Fig. 1D). Power spectral density estimates showed a prominent peak in the alpha-beta range for both patterns. The frequency at which this peak was located ("LVF frequency") varied considerably inside the HYP-LVF and LVF subgroups, but did not differ significantly between them (Fig. 1E).

3.3. Pre-ictal HFO densities and rates

We found that 15–10 s prior to seizure onset, HYP and LVF patients had different HFO subtype profiles (Fig. 2). While ripple density (Fig. 2C) and rate (pre-HYP: median 0.53 per s, range 0–2 per s; pre-LVF: median 0.20 per s, range 0–1.5 per s; $p = .09$, Wilcoxon rank sum test) did not differ significantly, fast ripple density (Fig. 2D) and rate (pre-HYP: median 0.16 per s, range 0–1.2 per s; pre-LVF: median 0 per s, range 0–0.47 per s; $p = .04$, Wilcoxon rank sum test) were higher before HYP than before LVF seizures. This difference did not reach significance with a more conservative permutation test (Table S1). To provide solid evidence for a role of pre-ictal fast ripples irrespective of spikes, spike-associated HFOs were excluded from the analyses presented above. Nonetheless, in these pre-HYP sections, we observed that HFOs tended to co-occur with pre-ictal spikes, even though we took great care to exclude "false" HFOs that are due to filtering of sharp transients (Bénar et al., 2010). If HFOs associated with spikes were also included, differences in fast ripple density (pre-HYP: median 1.4%, range 0–28%; pre-LVF: median 0%, range 0–2.2%; $p = .005$, Wilcoxon rank sum test) and rate (pre-HYP: median 0.4 per s, range 0–1.5 per s; pre-LVF: median 0 per s, range 0–0.47 per s; $p = .001$, Wilcoxon rank sum test) became more pronounced.

3.4. Ictal HFO densities and rates

During the initial 5 s after seizure onset (Fig. 3), we found, in analogy to our findings from the pre-ictal sections, no significant differences in ripple density (Fig. 3D) and rate (HYP: median 1.3 per s, range 0.5–3 per s; LVF: median 1.1 per s, range: 0–2.6 per s; $p = .35$, Wilcoxon rank sum test) between HYP and LVF onsets. Ripple density and rate were also similar in the two LVF subgroups (rate HYP-LVF: median 1.1 per s, range 0.3–5.5 per s; HYP-LVF vs. LVF p = .35, Wilcoxon rank sum test). Fast ripple density (Fig. 3E) and rate (HYP: median 1.1 per s, range: 0.33–2.7 per s; LVF: median 0.05 per s, range 0–2.9 per s; $p < .001$, Wilcoxon rank sum test), on the other hand, were higher during HYP onset than during LVF onset. Interestingly, higher rates and density of fast ripples were also found for the HYP-LVF pattern, when compared to LVF (Fig. 3E; rate HYP-LVF: median 1.75 per s, range 0–5.7 per s; HYP-LVF vs. LVF $p = .008$, Wilcoxon rank sum test).

3.5. HFO amplitude

During visual inspection of SEEG traces, we noticed that HFOs in HYP-LVF tended to have larger amplitudes than in LVF. To quantify this observation, we analyzed a parameter that we termed "HFO amplitude", which was defined as a frequency band-specific RMS (see above, "Data analysis" in the Methods section, for details). Both ripple and fast ripple amplitudes were consistently higher in HYP-LVF than in LVF (Fig. 4A, B). The amplitude of "background" activity in the ripple (80–250 Hz; $RMS_{non\text{-}ripple}$) or fast ripple (250–500 Hz; $RMS_{non\text{-}fast\ ripple}$) band, on the other hand, was not significantly different between the two subgroups.

Finally, we calculated the ratio (RMS_{HFO} / $RMS_{non\text{-}HFO}$) for ripples (Fig. 4C) and fast ripples (Fig. 4D) associated with HYP-LVF and LVF, thus comparing epochs with HFOs to epochs without HFOs not only for the ripple and fast ripple frequency bands, but also across a wide range of other spectral components. This ratio was highest in the 80–250 Hz band at the time of ripples and in the 250–500 Hz band at the time of fast ripples, as expected if our visually identified HFOs were indeed events characterized by an amplitude increase in their specific frequency band, and not resulting from a wideband effect. A progressive decrease was observed in neighboring to more distant spectral components; in the wide delta-to-gamma band, which is exclusively considered for routine EEG, no relevant HFO-associated amplitude increase was found.

4. Discussion

The main novel finding of this study is that in human MTLE patients, fast ripples are associated specifically with the HYP onset, in comparison to LVF onset seizures. This link was observed in pre-ictal intervals and not only during the HYP and LVF periods, but also when the low voltage fast activity that follows the hypersynchronous spikes (HYP-LVF) was compared to the standard LVF onset pattern. Furthermore, we report that both ripple and fast ripple amplitude are higher in HYP-LVF than in LVF.

4.1. Comparison with findings from animal models

We established that the association of fast ripples with HYP seizures, previously reported in two established rat models (Bragin et al., 1999; Lévesque et al., 2012; Bragin et al., 2005b), also exists in MTLE patients. However, we found no significant differences in ripple density or rate between HYP and LVF, as described in rodent models. Inferring a cellular mechanism from this finding is not trivial because, possibly due to differences in methodology, experimental data is heterogeneous. On the one hand, an increase in integrated amplitude of ripple range frequencies during the first second of HYP, but not of LVF seizures, was reported in the kainic acid model (Bragin et al., 2005b). On the other hand, in the pilocarpine model, more ripples than fast ripples were found during LVF seizures (Lévesque et al., 2012). Overlapping ripple and fast ripple events were discarded in that study; however, more recent work indicates that overlapping events were a minority (Lévesque et al., 2018). Interestingly, the main increase in ripple rate during LVF seizures occurred ~ 20–60 s after seizure onset in the pilocarpine-treated rats (Lévesque et al., 2012). During the initial 20 s after seizure onset, however, ripple rates were similar in LVF and HYP seizures, as is now also found in our data from humans. To analyze HFOs during the further course of HYP and LVF onset seizures may be an interesting objective of further investigations.

4.2. Impact on seizure classification in human MTLE patients

Classifying individual seizures and patients in human MTLE can be challenging. Although the distinction between HYP and LVF onsets is well accepted, individual expressions are diverse (Frauscher et al., 2017) and this was now confirmed by our quantitative results. We showed that the frequency of the rhythmic EEG discharge during the LVF pattern, HYP spike rate and a spike periodicity estimate varied considerably inside the two groups and frequently even within a single patient. This is consistent with previous reports of individuals with a variety of coexisting seizure onset patterns (Perucca et al., 2014;

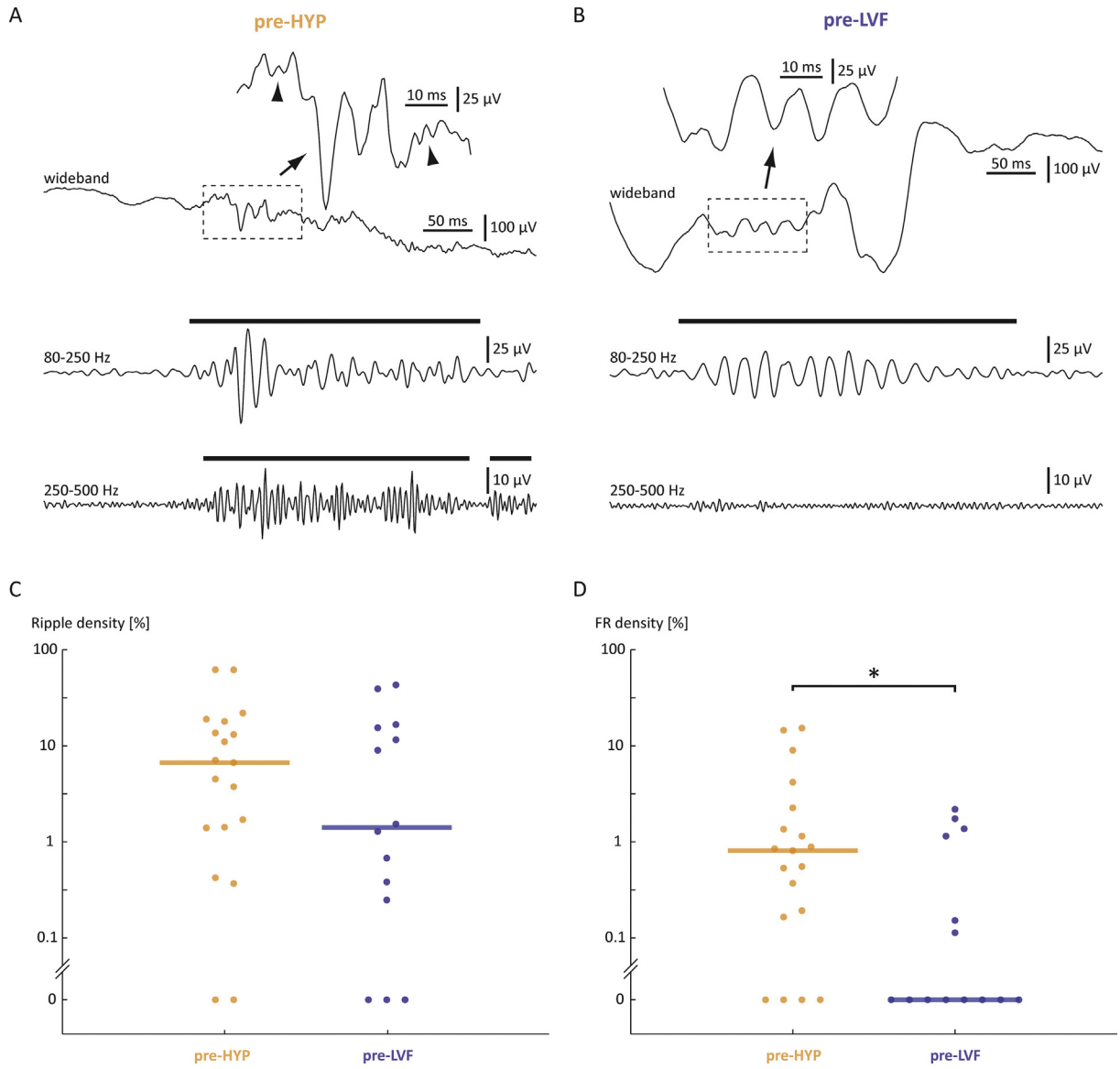

Fig. 2. Fast ripples are associated with HYP seizures before their actual onset. (A, B) SEEG recording from the deepest hippocampal electrode bipolar channel, 10–15 s prior to onset of the HYP (A, "pre-HYP") or LVF (B, "pre-LVF") pattern. (Top) Wideband (0.3–500 Hz), (middle) ripple band (80–250 Hz) and (bottom) fast ripple band (250–500 Hz) filtered traces. Horizontal bar above marks a visually identified ripple (A, B; middle) and fast ripple (A; bottom). Insets show a 50 ms interval selected from the wideband recording. Note that a mixed ripple (arrow) and fast ripple (arrowhead) is clearly visible in the pre-HYP sample, whereas the pre-LVF recording only has a "pure" ripple (arrow) without fast ripple component. (C, D) HFO density after exclusion of events associated with pre-ictal spikes. Each dot represents data from one seizure. Values greater than zero are plotted on a logarithmic scale and the y-axis is broken to visualize sections without HFOs. (C) Ripple density does not differ significantly between pre-HYP and pre-LVF (p = .35, Wilcoxon rank sum test). (D) Fast ripple density is higher in pre-HYP than in pre-LVF (p = .04, Wilcoxon rank sum test). This difference did not reach significance with a more conservative permutation test (Table S1). Note that prior to more than half of the LVF seizures, we found no fast ripples at all.

Spanedda et al., 1997). If only HYP and LVF are distinguished, the percentage of MTLE patients having both patterns ranges from 9% (Velasco et al., 2000) to 40% (Frauscher et al., 2017). This heterogeneity may be due to different inclusion criteria. For instance, in this study although we selected patients in order to get relatively homogeneous groups, both groups comprised a variety of etiologies and sometimes a bitemporal pathology.

Nevertheless, we consistently found that fast ripples are related to HYP rather than to LVF seizures. Importantly, when compared with LVF, fast ripple density and rate were also higher during the following HYP-LVF pattern. Moreover, ripple and fast ripple amplitude was higher during HYP-LVF than during LVF - possibly reflecting the involvement of larger neuronal assemblies, or a higher degree of synchrony. Our data may not exclude that some LVF onset seizures are initiated by HYP-like "microseizures" which are not seen due to limited spatial sampling or sensitivity of the macroelectrode recordings (Weiss et al., 2016; Stead et al., 2010). However, we provide evidence indicating that the HYP-LVF and LVF patterns are clearly different - in spite of appearing very similar upon visual examination. This conclusion is especially relevant if the onset of the HYP-LVF pattern is considered as the "true" seizure onset and HYP spikes are considered "pre-ictal", which has been proposed (Lévesque et al., 2012). Our findings rather support the view of HYP and LVF onset seizures as two entities, characterized by different initiation mechanisms: The association with fast ripples indicates out-of-phase firing of different pyramidal cell clusters (Foffani et al., 2007; Ibarz et al., 2010; Demont-Guignard et al., 2012) (see (Jiruska et al., 2017) for a review) with a predominance of excitatory currents (Shiri et al., 2016; Salami et al., 2015) in HYP

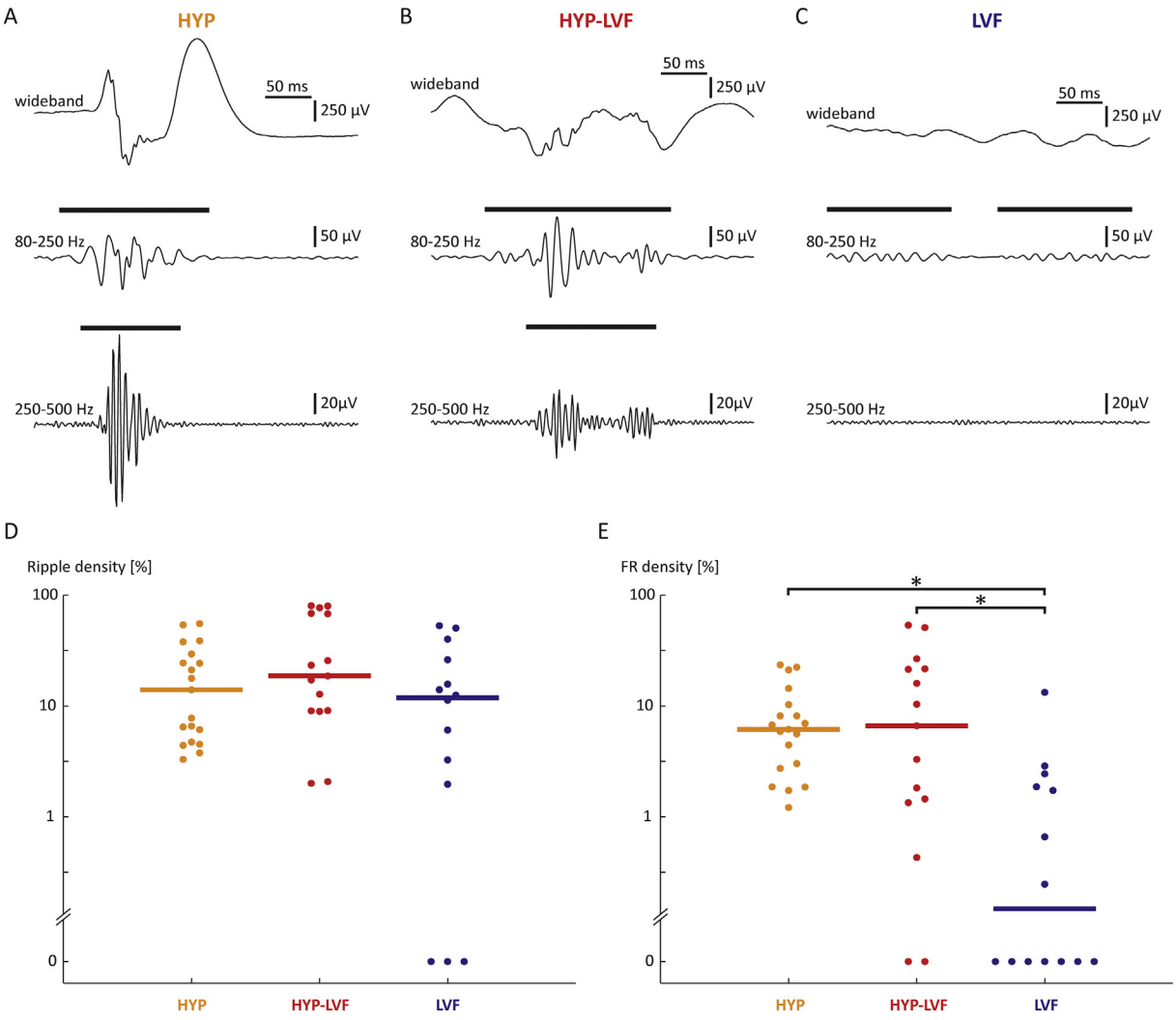

Fig. 3. Fast ripples are associated with the HYP and HYP-LVF patterns rather than with LVF. (A, B, C) SEEG recording from the deepest hippocampal electrode bipolar channel, during the HYP (A), HYP-LVF (B) and LVF (C) pattern. (Top) Wideband (0.3–500 Hz), (middle) ripple band (80–250 Hz) and (bottom) fast ripple band (250–500 Hz) filtered traces. Horizontal bar above marks visually identified ripples (A, B, C; middle) and a fast ripple (A, B; bottom). (D, E) HFO density. Each dot represents data from one seizure. A logarithmic scale is used to plot values greater than zero and the y-axis is broken to visualize sections without HFOs. (D) Ripple density does not differ significantly between HYP or HYP-LVF and LVF (HYP vs. LVF $p = .37$, HYP-LVF vs. LVF $p = .09$, Wilcoxon rank sum test). (E) Fast ripple density is higher in HYP and in HYP-LVF than in LVF (HYP vs. LVF $p < .001$, HYP-LVF vs. LVF $p = .007$, Wilcoxon rank sum test). Note that we found no fast ripples at all in half of the LVF seizures.

onsets. This mode of network activity seems to persist during subsequent HYP-LVF, whereas "pure" LVF is apparently generated by other mechanisms such as increased interneuron firing (Shiri et al., 2015; Shiri et al., 2016; Elahian et al., 2018).

4.3. Insights into the dynamics of HYP seizure generation

Interestingly, the association of fast ripples with HYP seizures was already found in our pre-ictal interval, i.e. 15–10 s prior to seizure onset. It would be desirable if this finding could be reproduced because differences did not reach significance with a more conservative permutation test, but it is at least consistent with a previous study reporting fast ripples of incrementally increasing power prior to HYP onsets (Weiss et al., 2016). Importantly, we defined seizure onset as the onset of the HYP and not, as is frequently preferred (Lévesque et al., 2012), the onset of the following HYP-LVF pattern. Therefore, and because pre-ictal spikes were excluded from our analysis, fast ripples might be regarded as events that are part of a genuine activity that builds up before HYP seizures. The fact that they do not predominate in interictal segments remote from seizures (Frauscher et al., 2017) also supports this view. In conclusion, the emergence of fast ripples may reflect the formation of a network activity that is closely linked to seizure generation. Whether parameters quantifying fast ripples correlate with the likelihood of occurrence of HYP seizures, as might be expected, would be an interesting question to tackle in future studies.

4.4. A note on "true" and "false" HFOs

HFO identification may be complicated by muscle artifacts and, more generally, by any wideband amplitude increase, which may be associated with sharp transients (Bénar et al., 2010). This applies especially to ictal EEG. Muscle artifacts, which can be visually identified based on their morphology (Zijlmans et al., 2011), were not observed in our dataset. This may be due to the fact that we analyzed SEEG and, importantly, only the three deepest bipolar channels. Sharp transients did occur. However, we reduced the risk of "false" HFO inclusion by analyzing only events with at least four oscillatory cycles. This strict criterion is well established (Perucca et al., 2014; Jacobs et al., 2010; Zijlmans et al., 2011), but more recently, only three cycles have been considered as also sufficient (Chu et al., 2017). We also show

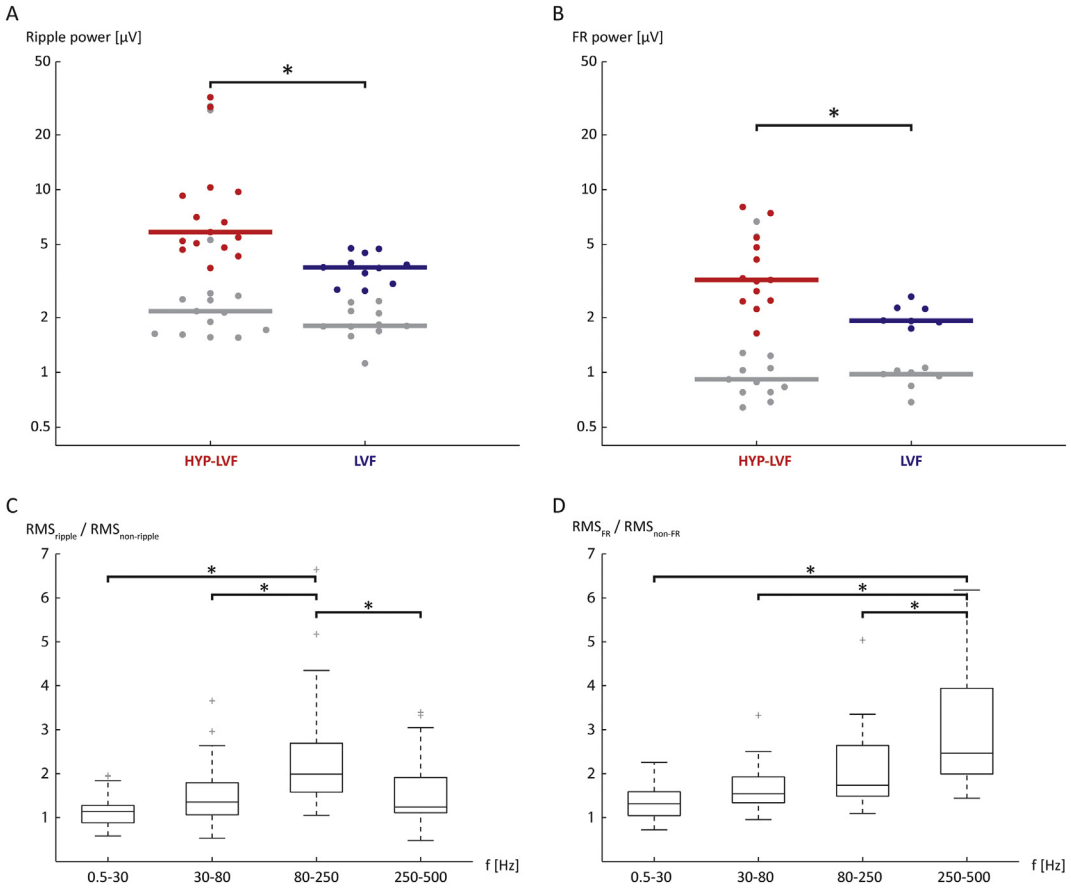

Fig. 4. Ripple and fast ripple amplitude is higher in HYP-LVF than in LVF. (A, B) HFO amplitude and $RMS_{non\text{-}HFO}$ (grey). Each dot represents data from one seizure. Ripple (A; $p < .001$, Wilcoxon rank sum test) and fast ripple (B; $p = .009$, Wilcoxon rank sum test) amplitude is higher in HYP-LVF than in LVF, whereas $RMS_{non\text{-}ripple}$ (A; $p = .18$, Wilcoxon rank sum test) and $RMS_{non\text{-}fast\ ripple}$ (B; $p = .87$, Wilcoxon rank sum test) does not differ significantly. (C, D) Ratio (RMS_{HFO} / $RMS_{non\text{-}HFO}$) at the time of visually identified ripples (C) and fast ripples (D) across a wide range of frequency bands. (C) RMS_{ripple} / $RMS_{non\text{-}ripple}$ during HYP-LVF and LVF is highest in the ripple band ($n = 26$ seizures; 80–250 Hz vs. 0.5–30 Hz $p < .001$, 80–250 Hz vs. 30–80 Hz $p < .001$, 80–250 Hz vs. 250–500 Hz $p < .001$, Wilcoxon matched-pairs signed-ranks test). (D) $RMS_{fast\ ripple}$ / $RMS_{non\text{-}fast\ ripple}$ is highest in the fast ripple band ($n = 20$ seizures; 250–500 Hz vs. 0.5–30 Hz $p < .001$, 250–500 Hz vs. 30–80 Hz $p < .001$, 250–500 Hz vs. 80–250 Hz $p = .008$, Wilcoxon matched-pairs signed-ranks test). These results demonstrate that at the time of ripples there was a specific increase in ripple amplitude, not a wideband amplitude increase; similarly for fast ripples.

examples of unfiltered SEEG with clearly visible HFOs without co-occurring sharp transients. Finally, we demonstrate that during HYP-LVF and LVF, marked HFOs were characterized by a pronounced amplitude increase in a characteristic rather narrow frequency band, contrary to what would be expected if the HFOs resulted from filtering a fast transient. Thus, in summary, we are confident that the vast majority of analyzed events were indeed “true” HFOs.

5. Outlook

If seizure-generating activity is accompanied by pre-ictal fast ripples, they might be useful for seizure prediction. However, from our data, an algorithm that solely relies on fast ripple density, rate or amplitude would not likely be sufficiently performant for clinical application. In multivariate approaches, though, fast ripples might be worth considering. To study the transition from HYP to HYP-LVF and the role of HFOs in this process might also be an interesting objective of future investigations.

Furthermore, correct classification of seizure onset patterns may be of relevance for individual patients. Evidence is scarce, but the HYP group seems to have a better post-surgical outcome (Schuh et al., 2000) and a smaller tendency to secondary generalization (Velasco et al., 2000; Bragin et al., 1999). Finally, dissection of the neuronal mechanisms underlying seizure generation might unveil novel targets for medical therapy and thus stimulate antiepileptic drug design.

Disclosure of conflicts of interest

None of the authors has any conflict of interest to disclose.

Ethical publication statement

We confirm that we have read the Journal's position on issues involved in ethical publication and affirm that this report is consistent with those guidelines.

Acknowledgements

This work was supported by the German Research Foundation (Research Fellowship to J. S.) and by the Canadian Institute of Health Research (grant FDN-143208 to J. G.).

Appendix A. Supplementary data

Supplementary data to this article can be found online at https://doi.org/10.1016/j.nbd.2019.03.030.

References

Avoli, M., de Curtis, M., Gnatkovsky, V., et al., 2016. Specific imbalance of excitatory/inhibitory signaling establishes seizure onset pattern in temporal lobe epilepsy. J.

Neurophysiol. 115, 3229–3237.
Bénar, C.G., Chauviere, L., Bartolomei, F., et al., 2010. Pitfalls of high-pass filtering for detecting epileptic oscillations: a technical note on “false” ripples. Clin. Neurophysiol. 121, 301–310.
Bragin, A., Engel Jr., J., Wilson, C.L., et al., 1999. Electrophysiologic analysis of a chronic seizure model after unilateral hippocampal KA injection. Epilepsia 40, 1210–1221.
Bragin, A., Wilson, C.L., Fields, T., et al., 2005a. Analysis of seizure onset on the basis of wideband EEG recordings. Epilepsia 46 (Suppl. 5), 59–63.
Bragin, A., Azizyan, A., Almajano, J., et al., 2005b. Analysis of chronic seizure onsets after intrahippocampal kainic acid injection in freely moving rats. Epilepsia 46, 1592–1598.
Chu, C.J., Chan, A., Song, D., et al., 2017. A semi-automated method for rapid detection of ripple events on interictal voltage discharges in the scalp electroencephalogram. J. Neurosci. Methods 277, 46–55.
Demont-Guignard, S., Benquet, P., Gerber, U., et al., 2012. Distinct hyperexcitability mechanisms underlie fast ripples and epileptic spikes. Ann. Neurol. 71, 342–352.
Elahian, B., Lado, N.E., Mankin, E., et al., 2018. Low-voltage fast seizures in humans begin with increased interneuron firing. Ann. Neurol. 84, 588–600.
Fisher, R.S., van Emde Boas, W., Blume, W., et al., 2005. Epileptic seizures and epilepsy: definitions proposed by the International League Against Epilepsy (ILAE) and the International Bureau for Epilepsy (IBE). Epilepsia 46, 470–472.
Foffani, G., Uzcategui, Y.G., Gal, B., et al., 2007. Reduced spike-timing reliability correlates with the emergence of fast ripples in the rat epileptic hippocampus. Neuron 55, 930–941.
Frauscher, B., von Ellenrieder, N., Dubeau, F., et al., 2017. Different seizure-onset patterns in mesiotemporal lobe epilepsy have a distinct interictal signature. Clin. Neurophysiol. 128, 1282–1289.
Ibarz, J.M., Foffani, G., Cid, E., et al., 2010. Emergent dynamics of fast ripples in the epileptic hippocampus. J. Neurosci. 30, 16249–16261.
Jacobs, J., Levan, P., Chatillon, C.E., et al., 2009. High frequency oscillations in intracranial EEGs mark epileptogenicity rather than lesion type. Brain 132, 1022–1037.
Jacobs, J., Zijlmans, M., Zelmann, R., et al., 2010. High-frequency electroencephalographic oscillations correlate with outcome of epilepsy surgery. Ann. Neurol. 67, 209–220.
Jirsch, J.D., Urrestarazu, E., LeVan, P., et al., 2006. High-frequency oscillations during human focal seizures. Brain 129, 1593–1608.
Jiruska, P., Alvarado-Rojas, C., Schevon, C.A., et al., 2017. Update on the mechanisms and roles of high-frequency oscillations in seizures and epileptic disorders. Epilepsia 58, 1330–1339.
Klausberger, T., Somogyi, P., 2008. Neuronal diversity and temporal dynamics: the unity of hippocampal circuit operations. Science 321, 53–57.
Klausberger, T., Magill, P.J., Marton, L.F., et al., 2003. Brain-state- and cell-type-specific firing of hippocampal interneurons in vivo. Nature 421, 844–848.
Lévesque, M., Salami, P., Gotman, J., et al., 2012. Two seizure-onset types reveal specific patterns of high-frequency oscillations in a model of temporal lobe epilepsy. J. Neurosci. 32, 13264–13272.
Lévesque, M., Wang, S., Gotman, J., et al., 2018. High frequency oscillations in epileptic rodents: are we doing it right? J. Neurosci. Methods 299, 16–21.
Memarian, N., Madsen, S.K., Macey, P.M., et al., 2015. Ictal depth EEG and MRI structural evidence for two different epileptogenic networks in mesial temporal lobe epilepsy. PLoS One 10, e0123588.
Ogren, J.A., Bragin, A., Wilson, C.L., et al., 2009. Three-dimensional hippocampal atrophy maps distinguish two common temporal lobe seizure-onset patterns. Epilepsia 50, 1361–1370.
Park, Y.D., Murro, A.M., King, D.W., et al., 1996. The significance of ictal depth EEG patterns in patients with temporal lobe epilepsy. Electroencephalogr. Clin. Neurophysiol. 99, 412–415.
Perucca, P., Dubeau, F., Gotman, J., 2014. Intracranial electroencephalographic seizure-onset patterns: effect of underlying pathology. Brain 137, 183–196.
Salami, P., Lévesque, M., Gotman, J., et al., 2015. Distinct EEG seizure patterns reflect different seizure generation mechanisms. J. Neurophysiol. 113, 2840–2844.
Schönberger, J., Draguhn, A., Both, M., 2014. Lamina-specific contribution of glutamatergic and GABAergic potentials to hippocampal sharp wave-ripple complexes. Front. Neural. Circuits 8, 103.
Schuh, L.A., Henry, T.R., Ross, D.A., et al., 2000. Ictal spiking patterns recorded from temporal depth electrodes predict good outcome after anterior temporal lobectomy. Epilepsia 41, 316–319.
Shiri, Z., Manseau, F., Lévesque, M., et al., 2015. Interneuron activity leads to initiation of low-voltage fast-onset seizures. Ann. Neurol. 77, 541–546.
Shiri, Z., Manseau, F., Lévesque, M., et al., 2016. Activation of specific neuronal networks leads to different seizure onset types. Ann. Neurol. 79, 354–365.
Spanedda, F., Cendes, F., Gotman, J., 1997. Relations between EEG seizure morphology, interhemispheric spread, and mesial temporal atrophy in bitemporal epilepsy. Epilepsia 38, 1300–1314.
Spencer, S.S., Guimaraes, P., Katz, A., et al., 1992. Morphological patterns of seizures recorded intracranially. Epilepsia 33, 537–545.
Stead, M., Bower, M., Brinkmann, B.H., et al., 2010. Microseizures and the spatiotemporal scales of human partial epilepsy. Brain 133, 2789–2797.
Tellez-Zenteno, J.F., Hernandez-Ronquillo, L., 2012. A review of the epidemiology of temporal lobe epilepsy. Epilepsy Res. Treat. 2012, 630853.
Velasco, A.L., Wilson, C.L., Babb, T.L., et al., 2000. Functional and anatomic correlates of two frequently observed temporal lobe seizure-onset patterns. Neural. Plast. 7, 49–63.
Weiss, S.A., Alvarado-Rojas, C., Bragin, A., et al., 2016. Ictal onset patterns of local field potentials, high frequency oscillations, and unit activity in human mesial temporal lobe epilepsy. Epilepsia 57, 111–121.
Weiss, S.A., Staba, R., Bragin, A., et al., 2019. Interneurons and principal cell firing in human limbic areas at focal seizure onset. Neurobiol. Dis. 124, 183–188.
Ylinen, A., Bragin, A., Nadasdy, Z., et al., 1995. Sharp wave-associated high-frequency oscillation (200 Hz) in the intact hippocampus: network and intracellular mechanisms. J. Neurosci. 15, 30–46.
Zijlmans, M., Jacobs, J., Zelmann, R., et al., 2009. High-frequency oscillations mirror disease activity in patients with epilepsy. Neurology 72, 979–986.
Zijlmans, M., Jacobs, J., Kahn, Y.U., et al., 2011. Ictal and interictal high frequency oscillations in patients with focal epilepsy. Clin. Neurophysiol. 122, 664–671.